Journal of Statistical Physics, Vol. 76, Nos. 1/2, 1994

Possible First-Order Transition in the Two-Dimensional Ginzburg–Landau Model Induced by Thermally Fluctuating Vortex Cores

Dierk Bormann[1] **and Hans Beck**[2]

Received September 10, 1993

We study the two-dimensional Ginzburg–Landau model of a neutral superfluid in the vicinity of the vortex unbinding transition. The model is mapped onto an effective interacting vortex gas by a systematic perturbative elimination of all fluctuating degrees of freedom (amplitude *and* phase of the order parameter field) except the vortex positions. In the Coulomb gas descriptions derived previously in the literature, thermal amplitude fluctuations were neglected altogether. We argue that if one includes the latter, the vortices still form a two-dimensional Coulomb gas, but the vortex fugacity can be substantially raised. Under the assumption that Minnhagen's generic phase diagram of the two-dimensional Coulomb gas is correct, our results then point to a first-order transition rather than a Kosterlitz–Thouless transition, provided the Ginzburg–Landau correlation length is large enough in units of a microscopic cutoff length for fluctuations. The experimental relevance of these results is briefly discussed.

KEY WORDS: Ginzburg–Landau model; XY model; two-dimensional Coulomb gas; Kosterlitz–Thouless transition; vortices; fluctuations; superconducting films.

1. INTRODUCTION

The critical behavior of two-dimensional (2D) systems with a continuous internal symmetry has been a most puzzling problem for a long time. Simple physical realizations are superfluid or superconducting thin films, which on a phenomenological level can both be described by a complex order parameter field Ψ, the boson or Cooper-pair "condensate wavefunction."

[1] Universität Augsburg, Institut für Physik, D-86135 Augsburg, Germany.
[2] Université de Neuchâtel, Institut de Physique, CH-2000 Neuchâtel, Switzerland.

822/76/1-2-25

The internal symmetry is then a $U(1)$ gauge symmetry acting on the phase of Ψ.

Early theoretical work showed that the "usual" criterion for superfluid order in 3D bulk systems[1] namely long-range order (LRO) of the field Ψ, is not satisfied in 2D films at any finite temperature.[2] The reason is low-energy phase fluctuations, the Goldstone modes related to the broken gauge symmetry, leading to Ψ correlations which decay algebraically to zero with distance. However, it was quickly realized[3] that this "quasi"-LRO was sufficient to ensure superfluidity. The correct criterion for superfluidity turned out to be rather a nonvanishing stiffness with respect to long-wavelength phase fluctuations (the *helicity modulus* Υ)[4] than true LRO in Ψ.

As a matter of fact, experimentally even very thin ^{4}He films of a *fraction* of an atomic layer showed clear signatures of superfluidity (see refs. in ref. 5). Two-dimensional superconductivity was predicted[6,7] for sufficiently "dirty" samples (high normal sheet resistance) and observed in continuous and granular thin films (see, e.g., refs. 8–11).

The nature of the transition from this superfluid phase to a high-temperature phase with exponentially decaying Ψ correlations was clarified by Berezinskiĭ[12] and Kosterlitz and Thouless (KT).[13,14] They realized the essential role of vortices, i.e., phase singularities with nonvanishing winding number ("vorticity"). The vortices interact logarithmically at large distances, and thus at low temperatures they appear as bound pairs of zero total vorticity only which do not change the algebraic decay of the Ψ correlations. However, at some finite temperature T_v, the largest vortex pairs in the system start to dissociate (unbind) by a collective screening mechanism, and the free vortices lead to an exponential decay of the correlations. (We use the notation T_v here in order to avoid confusion with a "conventional" critical point which will appear later.)

Usual phenomenological models of superconducting or superfluid films are the Ginzburg–Landau (GL) model or the XY ("planar rotator") model,[7,15] respectively (see also Section 2). The GL model is generally believed to provide an appropriate description of superconductors close to the bulk transition, since there is a microscopic derivation in the framework of Gor'kov theory (see, e.g., refs. 16). The XY model may be considered as the "phase-only" limit of the GL model, in which the modulus of Ψ is fixed and only its phase is allowed to fluctuate.[17] Together with the idea of thermally excited vortex loops, it has been successfully employed to describe the superfluid transition of ^{4}He in 3D[18] and 2D,[7,15] but there is no comparable microscopic justification as for the GL model in the case of superconductors.

Since the KT transition is essentially caused by the interacting vortex

system only, it appears in its purest form in a corresponding model system of pointlike particles in 2D with a logarithmic interaction, the 2D Coulomb gas (2DCG) model (for a review see, e.g., ref. 19). This model depends on two independent, dimensionless parameters, a temperature T^{CG} and a fugacity z^{CG} of the particles. The GL and XY models may then be thought of as particular realizations of the CG model, represented by particular $z^{CG}(T^{CG})$ lines.[19]

Based on the ideas of Kosterlitz and Thouless, a systematic renormalization group (RG) theory of the KT transition has been developed, usually starting from an XY or CG-type description.[20,21] In the CG picture, the KT RG equations are flow equations in the z^{CG}–T^{CG} plane; the $z^{CG}(T^{CG})$ line of a particular realization serves as initial condition of the RG flow. In the RG framework it could for instance be shown[22] that the helicity modulus has a finite value $\Upsilon(T \to T_v^{(-)}) \neq 0$ just below the transition and then drops *discontinuously* to zero. Furthermore, the ratio $2\pi\Upsilon(T)/k_B T$ tends to the *universal* value 4 at the transition $(T \to T_v^{(-)})$. This result may also be expressed in terms of pure CG quantities: general hydrodynamic arguments[23] show that the quantity $(\varepsilon_0(T^{CG})\, T^{CG})^{-1}$ (ε_0 being the $k \to 0$ limit of the CG dielectric function) corresponds *exactly* to the above-mentioned ratio $2\pi\Upsilon(T)/k_B T$ at all temperatures, in particular its discontinuity is the same.

This famous "universal jump" prediction is one of the central results of the KT RG theory and has been verified to an impressive degree by measurements on ^{4}He films[5] as well as by numerical work on XY-type models (see, e.g., refs. 24 and 25 and references therein) and CG-type models.[26] Quite convincing evidence for KT universal behavior has also been obtained for artificial superconductor networks, more specifically weakly coupled Josephson junction arrays (JJAs)[27] and wire networks,[28] which are both well described by XY-type models (see Section 2).

The situation for continuous superconducting films appears to be less clear. Experiments on high-T_c films (YBCO[10,11]) and dirty conventional films (Al,[8] In/InO[9]) provide rather good evidence for a discontinuous jump of the helicity modulus Υ at the transition; however, in both cases they seem to point to slightly *larger* values of this jump. (We note that in one case[10] the authors explain the observed behavior of Υ in a completely different way, namely by percolation effects due to the granularity of the film.)

Unfortunately, in the literature apparently no numerical results are available on the critical behavior of the 2D GL model. Usually, the 2D GL model is assumed[17,15] to have the same universal properties as the XY and CG models, since small-amplitude fluctuations of the order parameter Ψ have been shown[29] to be *irrelevant* in the RG sense. These fluctuations

are then neglected altogether, and one is left with a gas of GL vortices (termed "Ginzburg–Landau Coulomb gas" (GLCG) in the literature[30,19]; we will call it the "bare" GLCG, since fluctuations are not yet included) whose interaction is logarithmic at large distances and cut off roughly at the GL correlation length ξ. However, it is easily seen (see Section 2.1) that *right at* the expected vortex unbinding transition, the amplitude fluctuations can no longer be considered as weak and thus may well change the critical behavior.

A further, conceptual problem of the "bare" GLCG is that the *phase space division* Δ of a vortex is not well defined without additional arguments.[19] To get a rough idea of the size of Δ, one may argue that neglecting fluctuations at length scales $\lesssim\xi$ corresponds to a lattice regularization with lattice spacing $\sim\xi$. Consequently, the vortex phase space division is expected to be $\sim\xi^2$, since a vortex can be located at any of the plaquettes of the lattice. A more systematic approach to this question will be discussed at the end of this paper, in Section 4.4.

The above qualitative argument implicitly assumes that the only length scale which enters the problem is ξ; in particular the $z^{CG}(T^{CG})$ line should be *independent* of any microscopic cutoff length for fluctuations. In contrast, in the present paper we study precisely the influence of small-wavelength ($\lesssim\xi$) fluctuations on the transition. In doing so, we still assume that a description of the transition in terms of an effective interacting vortex gas is justified. We then take all thermal fluctuations systematically into account by a perturbative elimination of all degrees of freedom except the vortex positions. Our results will indicate that these fluctuations strongly *increase* the density of vortices at the transition or, in other words, they shift up the $z^{CG}(T^{CG})$ line.

Already KT in their original paper[14] noted that their approximations are justified only when the vortex system is dilute enough at the transition, i.e., when $z_v^{CG} = z^{CG}(T_v^{CG})$ is small enough. Outside the region of small z_v^{CG}, universality will hold only as far as the RG flow remains KT-like in a topological sense. On the other hand, Minnhagen[31] (see also refs. 19, 32, and 33) investigated the *whole* phase diagram of the 2D CG model by an extension to larger z^{CG} of the KT-Young self-consistent screening procedure[14,34] of deriving the RG equations. Minnhagen's modified RG equations are nonholonomous integrodifferential equations which in the small-z^{CG} limit reduce to the KT equations. Moreover, for small enough z^{CG} his corrections to the latter are *irrelevant* in the RG sense, i.e., Minnhagen's equations reproduce the same universal properties in this region. At larger values of z^{CG}, however, his equations predict a first-order transition line which ends at some critical point $(z_c^{CG}, T_c^{CG}) \approx (0.029, 0.204)$. The KT line joins the first-order line smoothly from below

at some point $(z_*^{CG}, T_*^{CG}) \approx (0.054, 0.144)$ (Fig. 1, qualitatively adapted from ref. 33). The superfluid transition is KT-like up to this point and first-order further above.

The first-order part probably may still be interpreted as a vortex unbinding transition, which in contrast to the KT transition involves the simultaneous dissociation of a *finite fraction* of all bound vortex pairs in the system. Its characteristics are nonuniversal; for instance, the jump of the above-mentioned quantity $[\varepsilon_0(T^{CG})\, T^{CG}]^{-1}$ depends on T_v^{CG} in the first-order part of the transition, and it is *larger* than the KT value 4.

In Fig. 1, we have included the $z^{CG}(T^{CG})$ lines representing the XY model and the "bare" GLCG, where for the latter we used the functional form proposed in ref. 35 (see also Section 2.3). The XY line definitely lies in the KT regime; there is thus no contradiction between the Minnhagen theory and the numerically well established fact (see references in refs. 24 and 25) that the XY model displays the universal properties of a KT transition. The GLCG line intersects both the KT and the first-order lines, but the superfluid transition is still KT-like. Our aim here is to argue that inclusion of fluctuations may shift the $z^{CG}(T^{CG})$ line even further up in the first-order regime.

However, the Minnhagen scenario must still be considered as somewhat speculative. Some effort has been made (see refs. 25 and 36 and

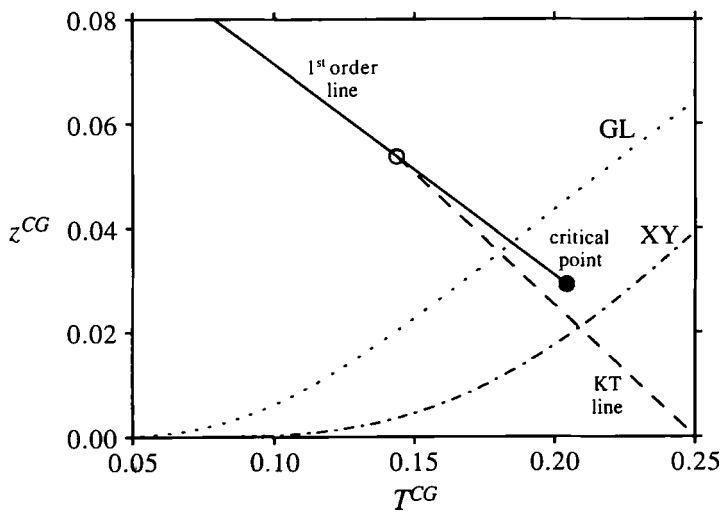

Fig. 1. Plot of Minnhagen's generic CG phase diagram.[31-33] Also shown are the $z^{CG}(T^{CG})$ relations [Eq. (18)] for the XY and GLCG models, using the parameters of Table I. In both cases, a KT-like vortex unbinding transition is predicted.

references therein) to decide whether a first-order transition exists in a modified XY model with a "truncated" cosine interaction between neighboring phase angles [which presumably also corresponds to a *higher* $z^{CG}(T^{CG})$ line than the XY one in Fig. 1], but the conclusions obtained by different authors are contradictory. Perhaps the strongest case in favor of the Minnhagen scenario could be made by Jonsson *et al.*[25] By a finite-size scaling analysis, they established the existence of a critical point *above* the KT line, which they identify with (z_c^{CG}, T_c^{CG}).

In summary, in this paper we try to treat the mapping of the 2D GL model on the corresponding interacting vortex gas in a somewhat more complete and systematic fashion than has been done so far in the literature. Thereby we find that fluctuations strongly enhance the vortex fugacity at the transition, which may drive the transition first-order, provided the Minnhagen scenario is correct.

The paper is organized as follows: in Section 2, we start with some general remarks about the GL description of superconducting films and networks, and also define our modified notion of the "Ginzburg–Landau vortex gas" (GLVG). The details of the main calculation are contained in Sections 3 and 4. The idea is to first investigate some kind of "saddle point" configuration of the field for given vortex positions (Section 3), which corresponds roughly to the "bare" GLCG discussed in the literature. In a second step, we include thermal fluctuations around this configuration in a Gaussian approximation (Section 4) and derive, as our central result, the $z^{CG}(T^{CG})$ relation for the GLVG. Section 5 contains a short summary and conclusions.

2. THE EFFECTIVE GINZBURG–LANDAU VORTEX GAS

2.1. Ginzburg–Landau Description of Superconducting Films

The starting point of this paper is the GL free energy functional of a complex order parameter field Ψ in 2D,

$$\mathscr{H}[\Psi] = \int d^2\mathbf{r} \left\{ \alpha |\Psi|^2 + \frac{\beta}{2} |\Psi|^4 + \gamma |\nabla\Psi|^2 \right\} \tag{1}$$

A *physical* system can be considered as 2D if the thickness of the film is smaller than some minimum wavelength of Ψ fluctuations, such that variations of Ψ perpendicularly to the plane are negligible. Note that we also omitted any coupling to the magnetic vector potential $\mathbf{A}$, i.e., (1) actually describes a *neutral* superfluid. Nevertheless, as argued in the introduction, such a local free energy is probably more appropriate for superconducting

films than for ^{4}He films. At the end of this section, we will indicate under which circumstaces the omission of a coupling to **A** can be justified.

$\mathscr{H}$ is used to define statistical mechanical quantities like the partition sum

$$Z \propto \int \mathscr{D}\Psi \, e^{-\mathscr{H}[\Psi]/k_B T} \tag{2}$$

The coefficients α, β, γ in $\mathscr{H}$ are in general temperature-dependent quantities: as usual, we assume that α vanishes at some "mean-field" critical temperature T_{c0}, and that $\alpha < 0$ for $T < T_{c0}$. Furthermore, for (2) to be defined, necessarily $\beta, \gamma > 0$. There is some freedom in the interpretation of the parameters α, β, γ and the order parameter field Ψ; usually, one chooses $\gamma = \hbar^2/2m_{\|}$, where $m_{\|}$ is the effective in-plane mass of the carriers (electrons or holes) and interprets $|\Psi|^2$ as the local density of carriers in the condensate. If we disregard boundaries, (1) assumes its minimum for the homogeneous field configuration $\Psi_\infty \equiv (|\alpha|/\beta)^{1/2}$ and for any other configuration which differs from Ψ_∞ by an arbitrary, spatially constant phase factor.

For later convenience and clarity we introduce a dimensionless order parameter field $\psi := (\beta/|\alpha|)^{1/2} \Psi$ normalized such that $\psi_\infty \equiv 1$. With

$$K := \frac{2\gamma |\alpha|}{\beta k_B T}, \qquad \xi := \left(\frac{\gamma}{|\alpha|}\right)^{1/2} \tag{3}$$

and

$$H[\psi] = \int d^2\mathbf{r} \left\{ \frac{1}{2\xi^2} (1 - |\psi|^2)^2 + |\nabla\psi|^2 \right\} \tag{4}$$

we can then rewrite the exponent of (2) as

$$\frac{\mathscr{H}[\Psi]}{k_B T} = \frac{K}{2} H[\psi] + \text{const} \tag{5}$$

where const stands for a ψ-independent term which is irrelevant for the thermodynamics. ξ is the GL "correlation" length which measures the length scale on which ψ relaxes to $\psi_\infty = 1$ away from a perturbation. We will see later that it is also the correlation length for thermal fluctuations of the amplitude $|\psi|$. Here K measures the stiffness of the ψ field over temperature and its inverse will later play the role of an effective statistical mechanical temperature. Note that $1/K$ and ξ both *diverge* as T approaches T_{c0} from below, since $|\alpha| \to 0$. Both effects tend to enhance fluctuations, so

if the KT transition is not preceded by some other transition to a disordered high-temperature phase, there must be a vortex unbinding transition at some temperature T_v *below* T_{c0}.

Expression (4) looks as if ξ were the only length scale in the problem and could be eliminated by a simple rescaling of all lengths, i.e., of $\mathbf{r}$. This is in fact the case in usual GL theory.[16] However, in order to obtain well-defined, finite results for statistical mechanical quantities like the partition sum (2) or ψ correlation functions, we have to limit the number of degrees of freedom by a UV regularization which introduces a second length scale. For definiteness, we may, for instance, put the model (4) on a square lattice with spacing a,

$$H[\psi] = \frac{a^2}{2\xi^2} \sum_i (1 - |\psi_i|^2)^2 + \sum_{\langle ij \rangle} |\psi_i - \psi_j|^2 \tag{6}$$

where $\sum_{\langle ij \rangle}$ denotes a sum over all pairs of nearest neighbor sites. Alternatively, we may supplement the continuum version (4) by the corresponding momentum cutoff prescription {i.e., all momenta in the Fourier representation of (4) restricted to the first Brillouin zone $[-\pi/a, \pi/a]^2$}. We will assume that both prescriptions are essentially equivalent and use them in parallel.

Expression (6) clearly shows that ξ/a is a second (besides K) dimensionless parameter which enters the model. In the limit $\xi \ll a$, the first term in (6) suppresses amplitude fluctuations of the order parameter away from the value $|\psi_i| \equiv 1$ and (6) reduces to the XY Hamiltonian,

$$H_{XY}[\psi] = \sum_{\langle ij \rangle} |e^{i\theta_i} - e^{i\theta_j}|^2 = 2 \sum_{\langle ij \rangle} [1 - \cos(\theta_i - \theta_j)] \tag{7}$$

where θ_i is the phase of ψ_i. In this respect, the XY model is the "phase-only" $\xi \to 0$ limit of the GL model. As mentioned in the introduction, its predictions agree well with measurements on Josephson junction arrays (JJAs) and superconducting wire networks. From our point of view, the reason for this success is that in these artificial networks the spacing of the underlying lattices provides a macroscopic cutoff length a which can be tuned independently of ξ. *Weakly* coupled networks,[27,28] which are preferred experimentally since their transition temperature is well separated from the bulk transition, then always lie in the regime $\xi \ll a$. Note that in a model of type (6) for weakly coupled JJAs, ξ is *not* equal to the bulk GL correlation length, but is usually much smaller (as a matter of fact, ξ^2/a^2 is essentially proportional to the Josephson coupling energy between two grains over the condensate energy of a grain). Consequently, there is no

contradiction to the fact that usually a is smaller than the bulk ξ in these systems.

The main points we want to stress now are the following:

1. In continuous superconducting films (as opposed to networks), ξ is *not* independent of a. In fact, it always obeys the inequality $\xi \gtrsim a$.
2. If $\xi \gtrsim a$, thermal amplitude fluctuations are quite strong close to the transition.

In the remainder of this paper, we will then analyze in detail the effect of these fluctuations and discuss in which way they may change the critical behavior.

In order to demonstrate point 2, we disregard for the moment the phase degrees of freedom and estimate the local fluctuations of the amplitude in a Gaussian approximation. An expansion of the potential term in the Hamiltonian (4) shows that amplitude fluctuations $\delta|\psi| = |\psi| - 1$ have a "mass" $2/\xi^2$. Therefore their mean square value at some "temperature" $1/K$ may be estimated as

$$\frac{\langle(\delta|\psi|)^2\rangle}{\langle|\psi|\rangle^2} \approx \frac{1}{2K}\int_{-\pi/a}^{\pi/a} \frac{d^2\mathbf{k}}{(2\pi)^2}\frac{1}{2/\xi^2+\mathbf{k}^2}$$

$$\approx \frac{1}{8\pi K}\int_0^{4\pi/a^2} \frac{d(k^2)}{2/\xi^2+k^2} = \frac{1}{8\pi K}\ln\left(1+2\pi\frac{\xi^2}{a^2}\right) \tag{8}$$

where in the second line we just have approximated the quadratic Brillouin zone by a circular one of the same area $(2\pi/a)^2$. At the presumed vortex unbinding transition, one expects the dimensionless "inverse temperature" K to be roughly of the order of 1, which implies that for $\xi \gtrsim a$ the $|\psi|$ fluctuations are of the same order of magnitude as its expectation value squared, $\langle|\psi|\rangle^2 \approx 1$.

To show that for superconducting films always $\xi \gtrsim a$ (point 1 above) we first have to understand the meaning of the cutoff a in this context. In fact, the Gor'kov derivation (see ref. 37, and also the reviews in refs. 16) of the GL functional (1) from BCS theory does not immediately yield a local form like (1), but involves integral kernels whose range plays the role of the cutoff a. Both a and the GL correlation length ξ can be calculated in this framework and one obtains roughly

$$\frac{\xi}{a} \approx \frac{1}{[\chi(1-T/T_{c0})]^{1/2}} \tag{9}$$

where $\chi \approx (1 + \hbar/2\pi k_B T\tau)^{-1}$ is a number <1 for dirty superconductors and $=1$ in the clean limit.[16] An immediate consequence of (9) is the validity of the asserted relation $\xi \gtrsim a$ at any temperature T. The ratio ξ/a diverges as T approaches T_{c0} from below; note that one usually even assumes $\xi \gg a$ to justify a local GL description. From BCS theory we can also estimate the value of ξ/a in the interesting region close to the presumed vortex unbinding transition: using (3), (9), one can show that

$$\frac{\xi}{a} \approx \left(\frac{\hbar^2 n_{2D}}{2m_{||} k_B T K}\right)^{1/2} \approx 210 \left(\frac{n_{2D}[\text{Å}^{-2}]}{T[\text{K}] \cdot K} \frac{m_e}{m_{||}}\right)^{1/2} \tag{10}$$

where n_{2D} [Å^{-2}] is the number of carriers in the film per Å^2 and $m_{||}$ their in-plane effective mass. At the transition ($T = T_v$), we assume again $K \approx 1$ and (10) yields a $\xi(T_v)$, which is appreciably larger than a unless the film has at the same time a high T_{c0}, low carrier density n_{2D}, and high in-plane carrier mass $m_{||}$ (note that these conditions may be realizable in films of high-T_c material whose thickness is a few unit cells).

The last point we want to address briefly in this subsection is the omission of a vector potential term in (1). *A priori*, such a coupling is important also in the absence of an external magnetic field, since thermal ψ fluctuations are accompanied by local supercurrents and therefore generate local magnetic fields.

The argument for the conventional scenario (no fluctuations except vortices) is well known[6,7] and goes as follows. It was shown by Pearl[38] that the logarithmic vortex–vortex interaction in superconducting films is magnetically screened at a length

$$\Lambda_s = \frac{2\lambda_L^2}{d} \tag{11}$$

where λ_L is the bulk London penetration depth and d the film thickness. For this reason, KT originally argued that a vortex unbinding transition should not occur in superconducting films since the logarithmic interaction at arbitrarily large distances is essential for the mechanism. However, it was noticed later[6,7] that for small d and sufficiently close to T_{c0} (note that λ_L diverges as $T \to T_{c0}$), Λ_s can become of the order of millimeters, i.e., comparable to typical sample sizes. Screening then should not wash out the transition to a larger extent than effects of finite system size and is therefore disregarded. The above authors restricted their argument to dirty films with a large λ_L ($T = 0$), but one can easily convince oneself using the GL

relationship $\lambda_L^2 = \hbar^2 c^2 \beta / 32\pi |\alpha| \gamma e^2$ that for *any* film, independent of its specifications,

$$\Lambda_s = \frac{(\hbar c/e)^2}{8\pi K k_B T} \approx \frac{1.2 \text{ cm}}{T[\text{K}] \cdot K} \tag{12}$$

At $T = T_v$, Λ_s should thus always be roughly of the order of 1 mm.

In this paper, we consider, in addition to vortices, the effect of amplitude and phase modulations, which are of course also accompanied by supercurrents. Screening effects lead in this case to an additional "mass" term $\sim 2/\Lambda_s^2$ for fluctuations; in particular, the massless phase (Goldstone) modes of the neutral superfluid become slightly massive. However, since our calculations will involve fluctuations of wavelength $\lesssim \xi$ only and since we can assume $\xi \ll \Lambda_s$ because of (12), we believe that we may disregard this effect, too. A more detailed discussion of this assumption may be interesting, but we will not further enter this question here.

2.2. Elimination of Short-Wavelength Fluctuations: Mapping on the Two-Dimensional Coulomb Gas

In this section, we outline the basic ideas of our approach. In particular, we try to clarify how the mapping of the 2DGL model at finite T on its associated vortex gas can be carried out in a systematic way.

Our aim is to study the presumed vortex unbinding transition which should show up in thermodynamic quantities like the partition sum (2). To this end we try to transform (2) into the statistical mechanical partition sum of an interacting vortex gas, i.e., we try to eliminate any degrees of freedom except the vortex positions.

On the technical level, the main step is to introduce a new lattice cutoff $\tilde{a} > a$ and to define an effective action $\tilde{S}[\psi_0]$ on a coarser lattice with constant $\tilde{a}$ (i.e., of the long-wavelength field components ψ_0) by integrating out the short-wavelength components ψ_1 which contain wave numbers between $\pi/\tilde{a}$ and π/a:

$$Z \propto \int_{0<k<\pi/\tilde{a}} \mathcal{D}\psi_0 \exp(\tilde{S}[\psi_0]) \tag{13}$$

$$\exp(\tilde{S}[\psi_0]) := \int_{\pi/\tilde{a}<k<\pi/a} \mathcal{D}\psi_1 \exp\left(-\frac{K}{2} H[\psi_0 + \psi_1]\right) \tag{14}$$

If $\tilde{a}$ is chosen large enough ($\tilde{a} \gtrsim a, \xi$) then we expect (13) to be dominated by "saddle point" configurations ψ_0 of H with vortices at given positions $\mathbf{R}_i$ (and with associated vorticities m_i) as constraints. The effective phase

space of the resulting vortex gas will be formed by the plaquettes (with area $\tilde{a}^2$) of the *coarser* lattice, which is important for the definition of the vortex entropy and thus for the thermodynamics. Nonsingular phase fluctuations ("spin waves") of wave numbers $k < \pi/\tilde{a}$ are also still contained in (13), but they decouple from the vortices as they do in the pure XY model and play no role in the transition, so we will disregard them (see also Section 4.2).

On the other hand, if $\tilde{a}$ is not much larger than $\max(a, \xi)$, then the effective action $\tilde{S}[\psi_0]$ may be determined to a reasonable approximation by a Gaussian approximation to the functional integral in (14). Then $\tilde{a}$ may be thought of as the smallest length scale on which vortices are well-distinguished objects. In Section 4.2 we will realize the infrared cutoff $\pi/\tilde{a}$ by a mass $2/\xi^2$ of the field ψ_1 ("soft" cutoff), where ξ is the GL correlation length. Both quantities will then turn out to be related by $\tilde{a}^2 = a^2 + 2\pi\xi^2$, which is in good agreement with our general discussion in the introduction and satisfies the above criteria.

Disregarding phase fluctuations of wave numbers $k < \pi/\tilde{a}$ as stated above, we can express the vortex part of (13) as

$$Z_v = \sum_N \frac{1}{N!} \sum_{\{m_i\}} \left(\prod_{i=1}^{N} \int \frac{d^2\mathbf{R}_i}{\tilde{a}^2} \right) \exp(\tilde{S}[\psi_0^{(N)}]) \tag{15}$$

where the determination of $\tilde{S}[\psi_0^{(N)}]$ as a function of the $\mathbf{R}_i$, m_i from (14) is the main technical task in this paper. N is the total number of vortices (of mutual separation $\gtrsim \tilde{a}$) in the system. We will later see that thermodynamically [i.e., in the partition sum (15)] only vorticities $m_i = \pm 1$ are important and, moreover, below T_v only "neutral" vortex configurations (obeying $\sum_i m_i = 0$).

As we will see in Section 4.3, for vortex distances much larger than $\tilde{a}$, $\tilde{S}[\psi_0^{(N)}]$ has an asymptotic behavior of the form

$$\tilde{S}[\psi_0^{(N)}] \sim \frac{1}{T^{CG}} \left(\sum_{i<j}^{N} m_i m_j \ln \frac{|\mathbf{R}_i - \mathbf{R}_j|}{\tilde{a}} + N\mu^{CG} \right) \tag{16}$$

i.e., it behaves as a neutral two-dimensional Coulomb gas (2DCG). The latter is generally defined by a partition sum of the form[19]

$$Z_v = \sum_N \frac{1}{N!} {\sum_{\{m_i\}}}' \left(\prod_{i=1}^{N} \int \frac{d^2\mathbf{R}_i}{\Delta} \right) \times \exp \frac{1}{T^{CG}} \left(\sum_{i<j}^{N} m_i m_j \ln_+ \frac{|\mathbf{R}_i - \mathbf{R}_j|}{R_c} + N\mu^{CG} \right) \tag{17}$$

where $\sum'_{\{m_i\}}$ now is a restricted sum over all *neutral* configurations of N

vortices with $m_i = \pm 1$. Here Δ is the "phase space division" of a CG charge, T^{CG} is the dimensionless CG temperature, and $-2\mu^{CG}$ may be interpreted as the creation energy of a neutral pair at distance R_c. Note that in (17) the interaction involves $\ln_+ x := \max(0, \ln x)$, i.e., it is cut off at smaller distances than R_c. Such a cutoff is essential for (17) to be well defined, but it can be realized in different ways.[19] It is easy to see that despite the appearance of the four parameters T^{CG}, μ^{CG}, Δ, and R_c, (17) actually depends only on T^{CG} and on the "fugacity"

$$z^{CG} = \frac{R_c^2}{\Delta} e^{\mu^{CG}/T^{CG}} \tag{18}$$

of the CG charges. The values which were used to draw the $z^{CG}(T^{CG})$ lines in Fig. 1 are taken from refs. 21 (XY model) and 19 and 35 ("bare" GLCG), and are collected in Table I. For the effective GLCG defined by (15), (16) we have by definition $\Delta = \tilde{a}^2$, but the short-distance cutoff is not yet specified in (16). We assume here $R_c \approx \tilde{a}$, such that simply $z^{CG} = \exp(\mu^{CG}/T^{CG})$. This is reasonable since $\tilde{a}$ is of the order of the vortex core size. To demonstrate that the results for $z^{CG}(T^{CG})$ are not too sensitive to the choice of R_c (nor presumably to the precise cutoff procedure), we have changed the values of the cutoff distance R_c in the case of the XY model and the "bare" GLCG by factors of 2 and 1/2. Note that there is an accompanying shift of μ^{CG}: the change to some other cutoff r_0' in (17) means that we have to replace $\ln_+(R/R_c) \mapsto \ln_+(R/R_c') + \ln(R_c'/R_c)$, which (using the charge neutrality condition) leads to

$$z \to z' = z \left(\frac{R_c'}{R_c}\right)^{2 - 1/2T^{CG}} \tag{19}$$

The results are shown in Fig. 2 and present no essential changes compared to Fig. 1; the effects with which we will be concerned later are much more pronounced.

Table I. Effective CG Parameters for the *XY* Model and for the "Bare" GLCG

Model	R_c	Δ	μ^{CG}
XY[21]	a	a^2	-0.809
GLCG[30,35]	2.24ξ	$16.4\xi^2$	-0.390

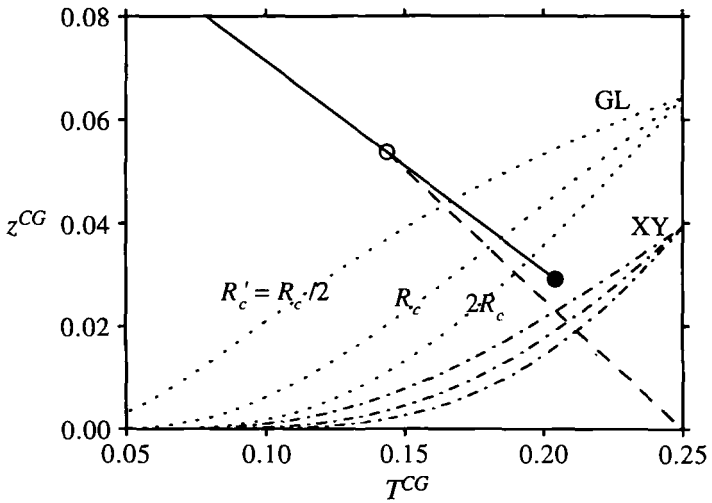

Fig. 2. Same as Fig. 1, but with several different values of the cutoff R_c of the vortex–vortex interaction [see Eq. (17)]. The qualitative properties of the vortex unbinding transition of the XY and GLCG models are not changed.

3. THE "SADDLE POINT" CONFIGURATION

As we argued in Section 2.2, the long-wavelength component ψ_0 of the field is essentially of the form of a "saddle point" configuration of H for given vortex positions $\mathbf{R}_i$ and vorticities m_i. So our first step will be a detailed investigation of these configurations and in particular of their energies $H[\psi_0]$. In Section 4 we will then proceed to calculate the effective action $\tilde{S}[\psi_0]$ of (14), by adding corrections due to thermal fluctuations around these saddle points.

Since in this section we are not considering fluctuations, we can work in the continuum limit $a \to 0$ [such that ξ is the only length scale of the Hamiltonian (4)] without encountering divergences. Only in Section 3.5 will we reintroduce a discrete lattice and discuss the way in which our results then are modified.

3.1. Separation of the Vortex Degrees of Freedom

In order to see how vortices, i.e., singularities of the phase with finite winding numbers ("vorticities"), can be imposed as constraints on the field ψ, we write the latter in terms of real fields ρ, θ ("amplitude" and "phase"),

$$\psi = \rho e^{i\theta} \tag{20}$$

and express the Hamiltonian (4) in terms of ρ, θ:

$$H[\rho, \theta] = \int d^2\mathbf{r} \left\{ \frac{1}{2\xi^2}(1-\rho^2)^2 + |\nabla\rho|^2 + \rho^2 |\nabla\theta|^2 \right\} \tag{21}$$

The phase gradient can be split into its longitudinal and transverse parts,

$$\nabla\theta = \nabla\vartheta - \mathbf{n} \times \nabla\Phi \tag{22}$$

where $\mathbf{n}$ is the unit vector normal to the plane. ϑ is a nonsingular phase field representing the "spin waves" and Φ is a "vortex potential" which satisfies the Poisson equation

$$\nabla^2\Phi(\mathbf{r}) = -2\pi \sum_i m_i \delta(\mathbf{r} - \mathbf{R}_i) \tag{23}$$

with pointlike integer "charges" (vorticities) m_i at the positions $\mathbf{R}_i$, corresponding to the singularities of the phase field θ (θ changes by $2\pi m_i$ upon going counterclockwise around $\mathbf{R}_i$). Φ is determined by (23) only up to a harmonic function; any harmonic contribution can, however, be absorbed into ϑ, so that we may choose the particular solution

$$\Phi(\mathbf{r}) = -\sum_i m_i \ln \frac{|\mathbf{r} - \mathbf{R}_i|}{\xi} \tag{24}$$

which finally renders the splitting (22) unique. In order to make the argument of the logarithm in (24) dimensionless we have introduced the only length scale ξ of the problem. Note, however, that for a "neutral" vortex configuration ($\sum_i m_i = 0$), Φ does not depend on ξ. The physical content of (22), (24) is that we have separated the vortex degrees of freedom (expressed by their positions $\mathbf{R}_i$ and vorticities m_i) from the remaining nonsingular phase configuration ϑ.

3.2. The Vortex Core Structure (One-Vortex Problem)

Besides the phase field which defines the vortices, our Hamiltonian contains the amplitude field ρ, which is strongly coupled to θ close to the vortex centers $\mathbf{R}_i$: far away from the centers ($\nabla\theta$ small) it is expected to have values $\rho \approx 1$; whereas it vanishes right at the vortex centers, $\rho(\mathbf{R}_i) = 0$, because otherwise the "vortex core" energies would diverge logarithmically in the continuum limit. We call *vortex core* the regions of size $\approx \xi$ around $\mathbf{R}_i$ where ρ significantly differs from 1. Since the structure of the core regions is essential for the following, we will investigate here in detail a

single isolated vortex of vorticity m centered at the origin. This subsection is sort of a summary of results taken from the literature which are relevant in our context.

Because of the isotropy of the problem we employ polar coordinates r, ϕ; in the saddle-point configuration of the Hamiltonian (21), the phase field is then (up to an additive constant which we choose equal to zero) given by

$$\theta_m(r, \phi) = m\phi \tag{25}$$

and the amplitude ρ_m is a function of r alone. Inserted in (21), this yields a reduced Hamiltonian of the one-vortex problem,

$$H_m[\rho_m] = \int dr\, 2\pi r \left\{ \frac{1}{2\xi^2}(1-\rho_m^2)^2 + \left(\frac{d\rho_m}{dr}\right)^2 + \frac{m^2}{r^2}\rho_m^2 \right\} \tag{26}$$

Its minimum solution is determined by a vanishing functional derivative with respect to ρ_m,

$$0 = -\frac{1}{4\pi r}\frac{\delta H_m}{\delta \rho_m(r)} = \frac{d^2\rho_m}{dr^2} + \frac{1}{r}\frac{d\rho_m}{dr} - \frac{m^2}{r^2}\rho_m + \frac{1}{\xi^2}\rho_m(1-\rho_m^2) \tag{27}$$

together with the boundary conditions

$$\rho_m(0) = 0, \qquad \rho_m(r) \to 1 \qquad \text{for} \quad r \to \infty \tag{28}$$

The solution $\rho_m(r)$ rises monotonically from 0 at $r=0$ to 1 at $r \to \infty$. To determine the asymptotic behavior of ρ_m at small and large r, one may proceed as follows:

1. $r \ll \xi$: here $\rho_m(r) \ll 1$, so we linearize (27) in ρ_m and insert an ansatz $\rho_m(r) \sim c_m(r/\xi)^\alpha$ with $\alpha > 0$ and c_m a numerical constant, which yields

$$0 \sim \frac{d^2\rho_m}{dr^2} + \frac{1}{r}\frac{d\rho_m}{dr} - \frac{m^2}{r^2}\rho_m \sim c_m(\alpha^2 - m^2)\frac{r^{\alpha-2}}{\xi^\alpha} \tag{29}$$

Thus $\alpha = |m|$, and c_m is a constant of order 1 which has to be determined numerically from the full solution of (27), (28). For $m=1$, ref. 30 gives

$$\lim_{r\to 0}\left(\frac{\xi^2}{2\pi r}\frac{d}{dr}\rho_{m=1}^2\right) = \frac{c_{m=1}^2}{\pi} = 0.108, \qquad \text{i.e.,} \quad c_{m=1} = 0.582 \tag{30}$$

2. $r \gg \xi$: here $u(r) := 1 - \rho_m(r) \ll 1$, so we linearize (27) in u and insert an ansatz $u(r) \sim c'_m (r/\xi)^\beta$ with $\beta < 0$:

$$0 \sim \frac{d^2u}{dr^2} + \frac{1}{r}\frac{du}{dr} + \frac{m^2}{r^2}(1-u) - \frac{2}{\xi^2}u$$

$$\sim c'_m(\beta^2 - m^2)\frac{r^{\beta-2}}{\xi^\beta} + \frac{m^2}{r^2} - 2c'_m\frac{r^\beta}{\xi^{\beta+2}} \tag{31}$$

For $r \to \infty$, the last two terms are the dominant ones, such that $\beta = -2$ and $c'_m = m^2/2$.

In conclusion, the asymptotic behavior of ρ_m is given by

$$\rho_m(r) \sim \begin{cases} c(r/\xi)^{|m|} & \text{for } r \ll \xi \\ 1 - \frac{1}{2}m^2(\xi/r)^2 & \text{for } r \gg \xi \end{cases} \qquad c_{m=1} = 0.582 \tag{32}$$

Sketches of ρ_m for $m = 1, 2$ are given in ref. 30. For later use we note that the first line of (32) together with $\theta_m = m\phi$ implies that close to the vortex center ($r \ll \xi$) the field $\phi_m = \rho_m e^{i\theta_m}$ has the simple power form

$$\psi_m(\hat{r}) \sim \begin{cases} c_m(\hat{r}/\xi)^{|m|} & \text{for } m > 0 \\ c_m(\hat{r}^*/\xi)^{|m|} & \text{for } m < 0 \end{cases} \tag{33}$$

where $\hat{r} = re^{i\phi}$ is a complex notation for the coordinate in the plane. Note in particular that the complex field is perfectly smooth even in the center of a vortex; a singularity only appears when one looks at the phase separately.

Now consider the different contributions to the total energy H_m, (26). Since for a circle-shaped system H_m diverges with the radius r_c as $\sim 2\pi m^2 \ln r_c$, we split off this size-dependent term:

$$H_m[\rho_m] \sim 2\pi\left(m^2 E_1(m) + E_2(m) + \frac{E_3(m)}{2} + m^2 \ln\frac{r_c}{\xi}\right) \tag{34}$$

for $r_c \gg \xi$, where

$$E_1(m) := \lim_{r_c \to \infty}\left(\int_0^{r_c} dr\,\frac{\rho_m^2}{r} - \ln\frac{r_c}{\xi}\right) = -\int_0^\infty dr\,\frac{d\rho_m^2}{dr}\ln\frac{r}{\xi} \tag{35}$$

$$E_2(m) := \int_0^\infty dr\, r\left(\frac{d\rho_m}{dr}\right)^2 \tag{36}$$

$$E_3(m) := \int_0^\infty dr\,\frac{r}{\xi^2}(1-\rho_m^2)^2 \tag{37}$$

The second expression for $E_1(m)$ follows by partial integration.

Table II. Numerical Values for the E Parameters of the One-Vortex Problem[a]

m	E_1	E_2	E_3
1	−0.806	0.279	1
2	—	0.416	4

[a] Equations (35)–(37). Taken from refs. 39 and 30. See explanation in text.

$E_3(m)$ can be calculated analytically by the following trick (we follow an idea of ref. 30): let ρ_m be the solution of (27), (28) and let $\rho_{m,\alpha}(r) := \rho_m(r/\alpha)$. Then the energy $H_m[\rho_{m,\alpha}]$ is minimum for $\alpha = 1$. To yield finite results it must again be regularized by a finite system radius $r_c \gg \xi$. After a variable change $r \mapsto \alpha r$ it reads

$$H_m[\rho_{m,\alpha}] = \int_0^{\alpha r_c} dr\, 2\pi r \left\{ \frac{\alpha^2}{2\xi^2}(1-\rho_m^2)^2 + \left(\frac{d\rho_m}{dr}\right)^2 + \frac{m^2}{r^2}\rho_m^2 \right\} \tag{38}$$

The minimum condition then implies that for $r_c \gg \xi$

$$0 = \frac{1}{2\pi}\frac{dH_m}{d\alpha}\bigg|_{\alpha=1} \sim m^2\rho_m(r_c)^2 - \int_0^{r_c} dr\, \frac{r}{\xi^2}(1-\rho_m^2)^2 \sim m^2 - E_3(m) \tag{39}$$

i.e.,

$$E_3(m) = m^2 \tag{40}$$

Once the system (27), (28) is numerically solved for a given m, the numbers $E_1(m)$ and $E_2(m)$ can also be evaluated. Reference 39 supplies a value $E_2(1) = 0.279$. This value is confirmed by ref. 30, which furthermore supplies $E_2(2)/4 + E_3(2)/8 = 0.604$, i.e., $E_2(2) = 0.416$ and $E_1(1) = -\ln 2.24 = -0.806$. The mentioned values of $E_i(m)$ are summarized in Table II.

3.3. Interaction of Vortices at Large Distances

Let us now calculate the interaction energy of a given vortex configuration defined by its potential Φ, (24), taking the core structure of the vortices into account. The interesting term in the Hamiltonian (21) is the third one, which couples ρ and θ. Inserting (22), we obtain

$$\int d^2\mathbf{r}\,\rho^2\,|\nabla\theta|^2 = \int d^2\mathbf{r}\,\rho^2\,|\nabla\vartheta - \mathbf{n}\times\nabla\Phi|^2$$

$$= \int d^2\mathbf{r}\,\rho^2\{|\nabla\vartheta|^2 - 2\,\nabla\vartheta\cdot(\mathbf{n}\times\nabla\Phi) + |\nabla\Phi|^2\}$$

$$= \int d^2\mathbf{r}\,\{\rho^2\,|\nabla\vartheta|^2 - 2\vartheta\mathbf{n}\cdot(\nabla\rho^2\times\nabla\Phi)$$

$$- \Phi(\rho^2\,\nabla^2\Phi + \nabla\rho^2\cdot\nabla\Phi)\} \tag{41}$$

The boundary terms appearing in the partial integration which leads to the third line of (41) would yield a *positive* contribution to the total energy which diverges logarithmically with the system size unless the vortex configuration is neutral ($\sum_i m_i = 0$), in which case they vanish. Nonneutral configurations are therefore thermodynamically suppressed (at least at low temperatures), and we consider here only neutral ones, for which (41) is correct.

To find the saddle point field configuration for given vortices we now have to minimize (21) [with (41) inserted] with respect to ρ and ϑ. Because of (23) and $\rho(\mathbf{R}_i) = 0$ the $\rho^2\nabla^2\Phi$ term vanishes identically. In general, the other terms interact in a complicated manner. However, we are interested at vortices at distances $\gtrsim\xi$ since we will treat the short-range fluctuations by other means in Section 4. Let us for simplicity assume that the smallest distance $|\mathbf{R}_i - \mathbf{R}_j|$ between any two vortices in the given configuration is $R \gg \xi$ and look for the leading terms in an expansion in ξ/R. The vortex cores are now well separated and in any of them ρ is expected to be given by the isotropic one-vortex solution of Section 3.2 plus a correction of the order $\mathcal{O}(\xi/R)$ (a justification will be given below). Together with (24) and by symmetry arguments this implies that $\nabla\rho^2\times\nabla\Phi$ is of order $\mathcal{O}(\xi/R)$, which in turn gives [see (41)] a saddle point configuration of ϑ of order $\mathcal{O}(\xi/R)$. Therefore (41) yields

$$\int d^2\mathbf{r}\,\rho^2\,|\nabla\theta|^2 = -\int d^2\mathbf{r}\,\Phi(\nabla\Phi\cdot\nabla\rho^2) + \mathcal{O}(\xi^2/R^2)$$

$$= -\sum_{i,j} m_i m_j \int d^2\mathbf{r}\,\frac{(\mathbf{r}-\mathbf{R}_j)\cdot\nabla\rho^2}{|\mathbf{r}-\mathbf{R}_j|^2}\ln\frac{|\mathbf{r}-\mathbf{R}_i|}{\xi} + \mathcal{O}\left(\frac{\xi^2}{R^2}\right) \tag{42}$$

In the second line, simply (24) has been inserted. The important contributions to the integral in (42) stem from a region of size $\mathcal{O}(\xi)$ around $\mathbf{R}_j$, the rest is again $\mathcal{O}(\xi^2/R^2)$. To calculate this integral, we may then assume that $\mathbf{R}_j = 0$ and replace ρ by the one-vortex solution with vorticity m_j centered

at the origin, ρ_{m_j} (see Section 3.2). We further have to distinguish two cases:

1. $i \neq j$; i.e., $\mathbf{R}_i = \mathbf{R}_i - \mathbf{R}_j =: \Delta\mathbf{R}$, $|\Delta\mathbf{R}| \geqslant R$. In this case the logarithm in (42) is dominated by a constant term $\ln(|\Delta\mathbf{R}|/\xi)$ and contains further terms $\mathcal{O}(\xi/R)$ which couple ρ in the core of vortex j to the other vortices. This leads to an *a posteriori* justification of the above assumption that the corrections to the one-vortex solution ρ_{m_j} around $\mathbf{R}_j$ are $\mathcal{O}(\xi/R)$. Again invoking symmetry arguments we finally obtain

$$\int d^2\mathbf{r}\, \frac{\mathbf{r}\cdot\nabla\rho^2}{|\mathbf{r}|^2} \ln\frac{|\mathbf{r}-\Delta\mathbf{R}|}{\xi} = 2\pi \ln\frac{|\Delta\mathbf{R}|}{\xi} \int_0^\infty dr\, \frac{d\rho_{m_j}^2}{dr} + \mathcal{O}\left(\frac{\xi^2}{R^2}\right)$$
$$= 2\pi \ln\frac{|\Delta\mathbf{R}|}{\xi} + \mathcal{O}\left(\frac{\xi^2}{R^2}\right) \tag{43}$$

since $\rho_{m_j}(r) \to 1$ for $r \to \infty$.

2. $i = j$; i.e., $\mathbf{R}_i = \mathbf{R}_j = \mathbf{0}$. This gives the strong "self-interaction" of the core amplitude of a vortex with its own phase configuration,

$$\int d^2\mathbf{r}\, \frac{\mathbf{r}\cdot\nabla\rho^2}{|\mathbf{r}|^2} \ln\frac{|\mathbf{r}|}{\xi} = 2\pi \int_0^\infty dr\, \frac{d\rho_m^2}{dr} \ln\frac{r}{\xi} + \mathcal{O}\left(\frac{\xi^2}{R^2}\right)$$
$$= -2\pi E_1(m) + \mathcal{O}(\xi^2/R^2) \tag{44}$$

We can now insert these results into (42), add the terms of (21) which contain ρ only, and express everything in terms of one-vortex quantities. So if $\psi_0 = \psi_0(\{\mathbf{R}_i, m_i\})$ is the minimum-energy field configuration with given vortices of vorticities m_i at positions $\mathbf{R}_i$, its energy is given by

$$H[\psi_0] = -4\pi \sum_{i<j} m_i m_j \ln\frac{|\mathbf{R}_i - \mathbf{R}_j|}{\xi} - 4\pi \sum_i \mu_{\mathrm{GL}}(m_i) + \mathcal{O}\left(\frac{\xi^2}{R^2}\right) \tag{45}$$

where

$$-2\mu_{\mathrm{GL}}(m) = m^2 E_1(m) + E_2(m) + \frac{m^2}{2} \tag{46}$$

To zeroth order in ξ/R, this is just the Hamiltonian of a *neutral two-dimensional Coulomb gas* of integer charges m_i whose core energy (or chemical potential μ_{GL}) depend on m_i. Note that in particular (45) contains *two-body* interactions only. We will later absorb the overall factor 4π in the effective Coulomb gas temperature.

For later use we also calculate the quantity $\xi^{-2}\int d^2\mathbf{r}\,(1-|\psi_0|^2)$ by

relating it to $H[\psi_0]$ in the following way: since ψ_0 is the minimum-energy field configuration for a given vortex configuration $\{\mathbf{R}_i, m_i\}$ as boundary conditions, the functional derivative $\delta H/\delta\psi_0(\mathbf{r})$ vanishes nowhere in space except at the vortex centers $\mathbf{r}=\mathbf{R}_i$. On the other hand, $\psi_0(\mathbf{r})$ itself has zeros precisely at the vortex centers, such that (with $\psi_0=\rho e^{i\theta}$)

$$0=\int d^2\mathbf{r}\,\psi_0\frac{\delta H}{\delta\psi_0}=\int d^2\mathbf{r}\left\{-\frac{1}{\xi^2}\rho^2(1-\rho^2)+|\nabla\rho|^2+\rho^2|\nabla\theta|^2\right\} \tag{47}$$

Now after adding $\xi^{-2}\int d^2\mathbf{r}\,(1-|\psi_0|^2)$ on both sides, the r.h.s. becomes almost identical to $H[\psi_0]$ apart from an additional factor of 2 in front of the E_3 integral [see (37)]. In analogy to (45) we therefore obtain

$$\begin{aligned}\int\frac{d^2\mathbf{r}}{\xi^2}(1-|\psi_0|^2)&=-4\pi\sum_{i<j}m_im_j\ln\frac{|\mathbf{R}_i-\mathbf{R}_j|}{\xi}\\&\quad-4\pi\sum_i\left[\mu_{\mathrm{GL}}(m_i)-\frac{1}{4}m_i^2\right]+\mathcal{O}\left(\frac{\xi^2}{R^2}\right)\\&=H[\psi_0]+\pi\sum_i m_i^2+\mathcal{O}(\xi^2/R^2)\end{aligned} \tag{48}$$

Identity (48) will be of central importance in Section 4 for the mapping of the full problem including fluctuations on a Coulomb gas.

At low temperatures $T<T_v$, the partition sum (15) will be dominated by configurations made out of bound vortex pairs of opposite vorticity. Furthermore, higher vorticities $|m|\geqslant 2$ have a much lower statistical weight than $|m|=1$ for pair distances $R\gg\xi$ because of their higher core energy and stronger binding [see (45)]. We therefore assume that they play no essential role in the vortex unbinding transition and restrict ourselves in the following to configurations with $m_i=\pm 1$.

3.4. The Functional Derivative $\delta H/\delta\psi_0$

The field configuration ψ_0 which we studied in Section 3.3 is no real saddle point of H since it is subject to the vortex boundary conditions defined by $\{\mathbf{R}_i, m_i\}$. However, clearly $\delta H/\delta\psi_0(\mathbf{r}_i)=0$ for $\mathbf{r}\notin\{\mathbf{R}_i\}$, so we expect something like $\delta H/\delta\psi_0(\mathbf{r}_i)\propto\delta(\mathbf{r}-\mathbf{R}_i)$ for $\mathbf{r}$ in the vicinity of $\mathbf{R}_i$. Since the functional derivative $\delta H/\delta\psi_0$ determines the *linear* energy of fluctuations away from ψ_0 (see Section 4), we will study it here in some detail. We consider again a neutral vortex configuration with minimum vortex distance $R\gg\xi$. Let us look at a neighborhood of the position $\mathbf{R}_i$ of the ith vortex and consider the particular fluctuation $\delta\psi_0$ generated by moving

vortex i by an infinitesimal vector $\delta\mathbf{R}_i$. Then (33) implies that for $|\mathbf{r}-\mathbf{R}_i| \ll \xi$ (assume for simplicity that $m>0$),

$$\psi_0(\mathbf{r}) \sim c_m \left(\frac{\hat{r}-\hat{R}_i}{\xi}\right)^m + \mathcal{O}\left(\frac{\xi}{R}\right) \tag{49}$$

with complex representations $\hat{r}$, $\hat{R}_i$ for $\mathbf{r}$, $\mathbf{R}_i$ as in (33). Consequently,

$$\delta\psi_0(\mathbf{r}) \sim -\frac{c_m}{\xi^m}(\hat{r}-\hat{R}_i)^{m-1}\,\delta\hat{R}_i + \mathcal{O}\left(\frac{\xi}{R}\right) \tag{50}$$

Now (45) implies that up to terms $\mathcal{O}(\xi^2/R^2)$ the total energy of the vortex system changes by an amount

$$\delta H[\psi_0] = -\mathbf{F}_i \cdot \delta\mathbf{R}_i = -\tfrac{1}{2}(\hat{F}_i^*\,\delta\hat{R}_i + \hat{F}_i\,\delta\hat{R}_i^*) \tag{51}$$

where

$$\mathbf{F}_i := 4\pi m_i \sum_{j(\neq i)} m_j \frac{\mathbf{R}_i-\mathbf{R}_j}{|\mathbf{R}_i-\mathbf{R}_j|^2} \tag{52}$$

is the total Coulomb force on the ith vortex, which is $\mathcal{O}(1/R)$. On the other hand, we can of course write

$$\delta H[\psi_0] = \int d^2\mathbf{r}\left(\frac{\delta H}{\delta\psi_0}\,\delta\psi_0 + \frac{\delta H}{\delta\psi_0^*}\,\delta\psi_0^*\right) \tag{53}$$

which after insertion of (50) leads by comparison with (51) to

$$\left(\frac{\hat{r}-\hat{R}_i}{\xi}\right)^{m-1}\frac{\delta H}{\delta\psi_0(\mathbf{r})} = \frac{\xi}{2c_m}\hat{F}_i^*\delta(\mathbf{r}-\mathbf{R}_i) + \mathcal{O}\left(\frac{\xi^2}{R^2}\right) \tag{54}$$

Note that the factor in front of the δ function is $\mathcal{O}(\xi/R)$, which will permit us to neglect the corresponding terms in the perturbation expansion of Section 4.

3.5. Interpolation to the *XY* Model

For convenience, we worked from the beginning of Section 3 in the continuum limit $a/\xi \to 0$. However, when we include fluctuations around the saddle-point configuration ψ_0 in Section 4, we will have to impose a finite lattice cutoff a. We will then want to expand around a suitable saddle point for *finite* a/ξ. For the fluctuation corrections of Section 4 we will take the discreteness into account mainly by a suitable cutoff in momentum space. The question addressed in this subsection is, what are the necessary modifications of (45), respectively (48), for finite a/ξ?

The asymptotic behavior of the vortex potential at large distances $R \gg \xi$, a will not be affected by the discreteness of the system. However, one expects an appreciable effect on vortex core energies since in the core regions the field ψ always varies on length scales down to the order of the lattice constant a. The extremest example is the XY or "plane rotator" model, which corresponds to the $\xi/a \to 0$ limit of (6), (4) where $\rho = |\psi| \equiv 1$. XY vortices are known to interact at distances $\gg a$ by a potential $4\pi \ln(R/a)$ and to have a well-defined *finite* core energy $4\pi\mu_{XY}$ (which is approximately given by half the creation energy of a vortex pair centered at neighboring plaquettes of the lattice), whereas (45) would predict a *logarithmic divergence* of μ_{XY} with ξ/a. More precisely, the energy calculated from (6), respectively (4), of a neutral pair at distance $R \gg a, \xi$ has the asymptotic forms

$$V_\xi(r) \sim \begin{cases} 4\pi\left(\ln\dfrac{R}{a} - 2\mu_{XY}\right) & \text{for} \quad \xi \ll a \\ 4\pi\left(\ln\dfrac{R}{\xi} - 2\mu_{\mathrm{GL}}\right) & \text{for} \quad \xi \gg a \end{cases} \tag{55}$$

where the respective chemical potentials are given by

$$\begin{aligned} -2\mu_{XY} &= \gamma + \frac{\ln 8}{2} \approx 1.617 \qquad \text{(see ref. 21)} \\ -2\mu_{\mathrm{GL}} &= E_1(1) + E_2(1) + \frac{1}{2} \approx -0.027 \end{aligned} \tag{56}$$

Here $\gamma = 0.5772$ is the Euler constant and $E_1(1)$, $E_2(1)$ are given in Table II. The factor in front of the logarithm in (55) is not affected by the lattice regularization.

We now look for a suitable interpolation formula for $V_\xi(R)$ which correctly reproduces both limits (55). Since we require an asymptotic behavior $V_\xi(R) \sim 4\pi \ln R + \text{const}$ for all ξ, it should be of the form

$$V_\xi(r) \sim 4\pi\{\ln(R/a) - 2\mu_{XY} - F(\xi^2/a^2)\} \tag{57}$$

where F is an interpolating function with the asymptotic behavior

$$F(0) = 0, \qquad F(X) \sim \tfrac{1}{2}\ln X + 2(\mu_{\mathrm{GL}} - \mu_{XY}) \qquad \text{for} \quad X \gg 1 \tag{58}$$

A simple realization of conditions (58) is

$$F(X) := \tfrac{1}{2}\ln(1 + Xe^{4(\mu_{\mathrm{GL}} - \mu_{XY})}) \approx \tfrac{1}{2}\ln(1 + 26.78X) \tag{59}$$

We tried to improve this simple guess for the interpolating function $F(X)$

by fitting the first derivative $F'(0)$ to the "true" value estimated by other means. However, this kind of improvement had no substantial effect on our final results, so we disregard it here. Finally, using expressions (57), (59), we can rewrite the "saddle-point" field energy (45) for vorticities $m_i = \pm 1$ in the interpolated form (for $R \gg \xi, a$)

$$H[\psi_0] \approx -4\pi \sum_{i<j} m_i m_j \ln \frac{|\mathbf{R}_i - \mathbf{R}_j|}{a} - 2\pi N(2\mu_{XY} + F(X)) + \mathcal{O}\left(\frac{\tilde{a}^2}{R^2}\right) \tag{60}$$

where N is the total number of vortices and $X = \xi^2/a^2$.

Starting from the lattice analog of (47), one can work out an equivalent interpolation formula for the integral (48), which, however, leads only to negligible corrections. We will therefore later simply use the expression (48) with the interpolated $H[\psi_0]$ inserted.

4. THERMAL FLUCTUATIONS AROUND THE "SADDLE POINT"

As we already argued in the introduction, we will identify the "saddle-point' field configuration ψ_0 with the long-wavelength components of the field ψ with wave numbers $|\mathbf{k}| < \pi/\tilde{a}$. Note that the latter still contain long-wavelength phase fluctuations which are absent in the "saddle-point" field configuration. However, as we will argue in Section 4.2, they are not important for the transition and can be disregarded. We will now calculate the effective action $\tilde{S}[\psi_0]$ [Eqs. (13), (14)] in a Gaussian approximation, i.e., we expand $H[\psi_0 + \psi_1]$ with respect to the fluctuations ψ_1 up to second order and treat their coupling to the vortices perturbatively.

4.1. Perturbational Treatment of Fluctuations

The first step is to expand the GL functional (4) around ψ_0:

$$\begin{aligned} H[\psi_0 + \psi_1] &= \int d^2\mathbf{r} \left\{ \frac{1}{2\xi^2} (1 - |\psi_0 + \psi_1|^2)^2 + |\nabla\psi_0 + \nabla\psi_1|^2 \right\} \\ &= H[\psi_0] + \int d^2\mathbf{r} \left\{ \frac{\delta H}{\delta \psi_0} \psi_1 + \frac{\delta H}{\delta \psi_0^*} \psi_1^* \right\} + \int d^2\mathbf{r}\, |\nabla\psi_1|^2 \\ &\quad + \int \frac{d^2\mathbf{r}}{2\xi^2} \{2(2|\psi_0|^2 - 1)|\psi_1|^2 + \psi_0^{*2}\psi_1^2 + \psi_0^2\psi_1^{*2}\} \\ &\quad + \int \frac{d^2\mathbf{r}}{2\xi^2} \{2(\psi_0^*\psi_1 + \psi_0\psi_1^*)|\psi_1|^2 + |\psi_1|^4\} \end{aligned} \tag{61}$$

where the terms are ordered in ascending order in ψ_1. In a vortex-free configuration we would have $|\psi_0| \equiv 1$ and the linear terms in ψ_1 would vanish. Now write again $\psi_0 = \rho_0 e^{i\theta_0}$, take all terms which are quadratic in ψ_1 (and ψ_1^*), replace ρ_0 by 1, and collect them in some "free" fluctuation Hamiltonian H_0. Now (61) can be rewritten as

$$H[\psi_0 + \psi_1] = H[\psi_0] + H_0[\psi_1] + H_I[\rho_0, \theta_0, \psi_1] \tag{62}$$

where

$$H_0[\psi_1] = \int d^2\mathbf{r} \left\{ \frac{1}{2\xi^2} [2|\psi_1|^2 + (e^{-i\theta_0}\psi_1)^2 + (e^{i\theta_0}\psi_1^*)^2] + |\nabla\psi_1|^2 \right\} \tag{63}$$

is the free fluctuation Hamiltonian and all remaining terms are collected in the "perturbation"

$$H_I[\rho_0, \theta_0, \psi_1] = \int d^2\mathbf{r} \left\{ \frac{\delta H}{\delta \psi_0} \psi_1 + \frac{\delta H}{\delta \psi_0^*} \psi_1^* \right\}$$
$$- \int \frac{d^2\mathbf{r}}{2\xi^2} (1 - \rho_0^2)\{4|\psi_1|^2 + (e^{-i\theta_0}\psi_1)^2 + (e^{i\theta_0}\psi_1^*)^2\} + \mathcal{O}(\psi_1^3) \tag{64}$$

which describes the coupling of fluctuations to vortex cores and vanishes in a vortex-free configuration. Closer examination of (63) reveals that, locally, the field ψ has one massive and one massless component, the orientation of the local reference frame being determined by the phase θ_0 of the "saddle-point" configuration. More precisely, the real and imaginary parts of the "gauge-transformed" field $e^{-i\theta_0}\psi_1$ correspond to massive amplitude fluctuations (mass $2/\xi^2$) and massless phase fluctuations, respectively. In two dimensions the real-space propagator of a massless field is infrared divergent, which causes serious problems in a perturbation expansion. In the next section, we will therefore be concerned with the infrared regularization of the phase fluctuations.

4.2. Infrared Regularization of Phase Fluctuations

In order to understand the physical role of long-wavelength phase fluctuations, we return to the representation (21), (41) of H, where phase fluctuations are described by a field ϑ. The terms which couple to ϑ in (41) only contain wavelengths $\lesssim \xi$, so long-wavelength components $\vartheta_{\mathbf{k}}$ with $|\mathbf{k}| \ll 1/\xi$ decouple from the vortices and therefore play no role in the vortex unbinding transition (note that in the continuum XY limit $\xi \ll a$, ϑ

decouples *completely*!). This leads us to assume that all components with $|\mathbf{k}| < \pi/\tilde{a}$ are irrelevant and can be disregarded. We will then treat the components with $\pi/\tilde{a} < |\mathbf{k}| < \pi/a$ perturbatively. For technical reasons it is convenient to realize this infrared momentum cutoff $\pi/\tilde{a}$ in a "soft" way, by assigning a *mass* to the phase fluctuations in (63). For simplicity we choose this mass to be the same ($=2/\xi^2$) as for the amplitude fluctuations, such that (63) is replaced by the simpler, translationally invariant expression with isotropic mass matrix

$$\tilde{H}_0[\psi_1] = \int d^2\mathbf{r} \left(\frac{2}{\xi^2} |\psi_1|^2 + |\nabla \psi_1|^2 \right) \tag{65}$$

(We will argue in Section 4.4 that the relation between "hard" and "soft" cutoffs is given by $\tilde{a}^2 = a^2 + 2\pi\xi^2$.) With this modification, the Hamiltonian (62) now describes a system of interacting vortices together with a massive, harmonic field ψ_1 [made up of amplitude and phase fluctuations and described by (65)] which is scattered by the vortex cores. In the calculation of the effective action (14) we may now integrate over *all* components $\psi_{1\mathbf{k}}$ with $|\mathbf{k}| < \pi/a$ since the infrared cutoff is taken into account by the mass.

The free propagator corresponding to Hamiltonian (65) is given by

$$\langle \psi_1(\mathbf{r})\, \psi_1^*(\mathbf{0}) \rangle = \frac{\int d[\psi_1]\, \psi_1(\mathbf{r})\, \psi_1^*(\mathbf{0}) \exp(-\tilde{H}_0)}{\int d[\psi_1] \exp(-\tilde{H}_0)} = \frac{2}{K} G_0(\mathbf{r}) \tag{66}$$

where

$$G_0(\mathbf{r}) = \int \frac{d^2\mathbf{k}}{(2\pi)^2} G_0(\mathbf{k})\, e^{i\mathbf{k}\cdot\mathbf{r}} \tag{67}$$

$$G_0(\mathbf{k}) = \frac{1}{2/\xi^2 + \mathbf{k}^2} \tag{68}$$

For later use in the perturbational expansion, we derive here some properties of G_0. The local mean square value of ψ_1 is closely related to the fluctuations already calculated in Eq. (8),

$$\frac{K}{2} \langle |\psi_1^2| \rangle = G_0(\mathbf{r} = \mathbf{0}) = \int \frac{d^2\mathbf{k}}{(2\pi)^2} \frac{1}{2/\xi^2 + \mathbf{k}^2} \approx \frac{1}{4\pi} \ln(1 + 2\pi X) \tag{69}$$

where we again used the notation $X = \xi^2/a^2$. More generally, one can show that

$$G_0(\mathbf{r}) \approx \begin{cases} \dfrac{1}{4\pi} \ln(1 + 2\pi X) & \text{for } \mathbf{r} = \mathbf{0} \\ -\dfrac{1}{2\pi} \ln \dfrac{|\mathbf{r}|}{\xi} & \text{for } a \leqslant |\mathbf{r}| \leqslant \xi \\ 0 & \text{for } |\mathbf{r}| > a, \xi \end{cases} \tag{70}$$

where the second line is relevant only if $a < \xi$. The n-fold convolution of G_0 with equal arguments at the ends can be calculated in analogy to (69),

$$\begin{aligned} (G_0^{n+1})(\mathbf{r} = \mathbf{0}) &= \int_2 \cdots \int_{n+1} G_0(1, 2)\, G_0(2, 3) \cdots G_0(n+1, 1) \\ &= \int \frac{d^2\mathbf{k}}{(2\pi)^2} G_0(\mathbf{k})^{n+1} \\ &\approx \frac{1}{4\pi} \int_0^{4\pi/a^2} \frac{d(k^2)}{(2/\xi^2 + k^2)^{n+1}} \\ &= \frac{1}{4\pi n} \left\{ \left(\frac{2}{\xi^2} \right)^{-n} - \left(\frac{4\pi}{a^2} + \frac{2}{\xi^2} \right)^{-n} \right\} \end{aligned} \tag{71}$$

which is never larger than its $\xi \gg a$ limit:

$$(G_0^{n+1})(\mathbf{r} = \mathbf{0}) \leqslant \frac{\xi^{2n}}{4\pi n 2^n} \tag{72}$$

We write out the particular case $n = 1$ explicitly:

$$\int d^2\mathbf{r}\, G_0(\mathbf{r})^2 \approx \frac{\xi^2}{4} \frac{X}{1 + 2\pi X} \leqslant \frac{\xi^2}{8\pi} \tag{73}$$

4.3. Diagrammatics

We will now calculate the effective action $\tilde{S}[\psi_0]$ [Eq. (14)] by diagrammatic perturbation theory, starting from the decomposition (62),

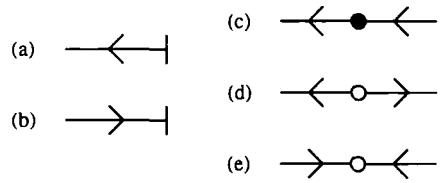

Fig. 3. Diagrams corresponding to the interaction term H_I of the Hamiltonian, Eq. (74).

(64), (65) of the original Hamiltonian. The propagator of the theory is $(K/2)\,G_0$, defined by (67), (68). Furthermore, up to $\mathcal{O}(\psi_1^2)$ the interaction term $-(K/2)\,H_I$ is represented by a sum of the diagram elements shown in Fig. 3, with combinatoric factors of 1/2 for the symmetric diagrams (d) and (e). The corresponding analytic expressions read

$$\begin{aligned}
(\mathrm{a}) &= -\frac{K}{2}\int \frac{\delta H}{\delta \psi_0^*}\,\psi_1^* \\
(\mathrm{b}) &= -\frac{K}{2}\int \frac{\delta H}{\delta \psi_0}\,\psi_1 \\
(\mathrm{c}) &= \frac{K}{\xi^2}\int (1-\rho_0^2)\,|\psi_1|^2 \\
(\mathrm{d}) &= \frac{K}{2\xi^2}\int (1-\rho_0^2)\,e^{2i\theta_0}\psi_1^{*2} \\
(\mathrm{e}) &= \frac{K}{2\xi^2}\int (1-\rho_0^2)\,e^{-2i\theta_0}\psi_1^2
\end{aligned} \tag{74}$$

respectively. Omission of terms of higher order than $\mathcal{O}(\psi_1^2)$ just means that we are working in the Gaussian approximation. The perturbation series for the effective action $\tilde{S}[\psi_0]$ [Eq. (14)] may now be expressed as $-(K/2)\,H[\psi_0]$ plus the sum of the diagrams shown in Fig. 4 with the appropriate combinatorial factors (plus higher-order terms to be discussed in a moment). We calculate these different diagrams separately, keeping only the "leading" terms, i.e., those which contribute to the logarithmic interaction or the chemical potential in $H[\psi_0]$ [Eq. (45)], and omitting terms $\mathcal{O}(\xi^2/R^2)$.

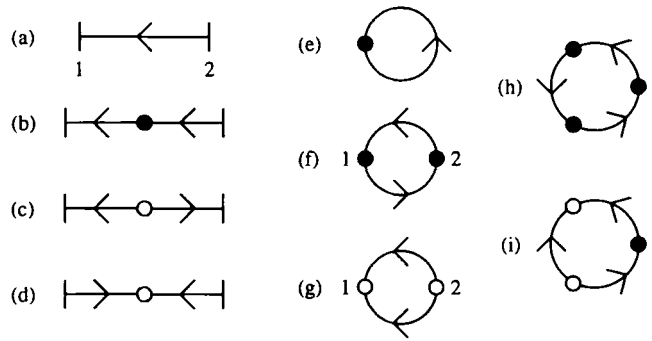

Fig. 4. Diagrams corresponding to the Gaussian approximation of the effective action $\tilde{S}[\psi_0]$.

Consider first the "chain" diagrams in Fig. 4:

$$(a) = \frac{K}{2}\int_1\int_2 G_0(1,2)\frac{\delta H}{\delta\psi_0(1)}\frac{\delta H}{\delta\psi_0^*(2)}$$
$$\approx \frac{K}{2}G_0(\mathbf{r}=\mathbf{0})\left(\frac{\xi}{2c_1}\right)^2\sum_i |\mathbf{F}_i|^2 = \mathcal{O}\left(\frac{\xi^2}{R^2}\right) \tag{75}$$

where we used (54) for $m=1$. Similar arguments show that all of the "chain" diagrams [(b), (c), (d), and "longer" ones] are likewise $\mathcal{O}(\xi^2/R^2)$ and they will therefore be neglected.

The "loop" diagrams (e), (f),... in Fig. 4 are more interesting. The only one which gives a contribution to the logarithmic term in the vortex interaction is diagram (e):

$$(e) = 2G_0(\mathbf{r}=\mathbf{0})\,\xi^{-2}\int(1-\rho_0^2)$$
$$\approx \frac{1}{2\pi}\ln(1+2\pi X)(H[\psi_0]+\pi N)+\mathcal{O}\left(\frac{\tilde{a}^2}{R^2}\right) \tag{76}$$

where we used (69), (48) for $m_i=\pm 1$ and N is the total number of vortices in ψ_0. The higher-order loops all give *positive* contributions to the vortex chemical potential. The most important of them is

$$\frac{1}{2}\times(f) = \frac{2}{\xi^4}\int_1\int_2 G_0(1,2)^2\,[1-\rho_0(1)^2][1-\rho_0(2)^2]$$
$$\lesssim 2\xi^{-2}\left(\int G_0^2\right)\xi^{-2}\int(1-\rho_0^2)^2 \approx \pi N\frac{X}{1+2\pi X}+\mathcal{O}\left(\frac{\tilde{a}^2}{R^2}\right) \tag{77}$$

where the $\lesssim$ sign expresses that we used a Schwarz inequality to estimate the integral at the l.h.s., and we used (73), (37), (40) to evaluate the r.h.s. (note that we took the symmetry factor of the diagram already into account). Similarly we treat the next diagram,

$$\frac{1}{4}\times(g) = \frac{1}{4\xi^4}\int_1\int_2 G_0(1,2)^2\,[1-\rho_0(1)^2][1-\rho_0(2)^2]\cos 2[\theta_0(1)-\theta_0(2)]$$
$$\lesssim \frac{\pi N}{8}\frac{X}{1+2\pi X}+\mathcal{O}\left(\frac{\tilde{a}^2}{R^2}\right) \tag{78}$$

where in addition we neglected the cosine factor on the l.h.s., which is of course a more serious approximation; however, the contribution of (78) is smaller than that of (77) by a factor of 1/8 in any case, so we neglect this

error. We note that both approximations (77), (78) would be good in a limit where the range of $G_0(\mathbf{r})^2$ is much smaller than that of $[1-\rho_0(\mathbf{r})^2]$, but (70), (32) imply that both ranges are actually of the order of ξ.

The dominant class of terms in the whole series is given by loop diagrams of the form shown in Fig. 5 with $n+1$ nodes, $n=1, 2,...$, and a symmetry factor of $1/(n+1)$ [the first two are (f) and (h) in Fig. 4]. An upper limit to the contribution of any of these diagrams may be found by again using a Schwarz inequality as above, and directly applying (72):

$$\begin{aligned}\frac{1}{n+1}\times(\text{Fig. 5}) &= \frac{1}{n+1}\left(\frac{2}{\xi^2}\right)^{n+1}\int_1\cdots\int_{n+1} G_0(1,2)\cdots G_0(n+1,1)\\ &\quad\times[1-\rho_0(1)^2]\cdots[1-\rho_0(n+1)^2]\\ &\lesssim \frac{1}{2\pi n(n+1)}\,\xi^{-2}\int(1-\rho_0^2)^{n+1}\end{aligned}\tag{79}$$

The integrals on the r.h.s. monotonically tend to zero with increasing n and their coefficients alone form a rapidly converging series with sum $1/2\pi$ [for comparison, the first term corresponding to diagram (f) in Fig. 4 already contributes $1/4\pi$]. Since we already overestimated the contributions of (f), (g), we therefore neglect all higher "loop" diagrams and hope for the best. We will see in the next subsection that any further positive contribution to the vortex chemical potential *amplifies* the observed effect and thereby strengthens our argument anyway. Putting everything together, we now obtain

$$\begin{aligned}\tilde{S}[\psi_0] &= -\left\{\frac{K}{2}-\frac{1}{2\pi}\ln(1+2\pi X)\right\}H[\psi_0]+\frac{N}{2}\ln(1+2\pi X)\\ &\quad+2\pi N\left(\frac{1}{2}+\frac{1}{16}\right)\frac{X}{1+2\pi X}+\mathcal{O}\left(\frac{\tilde{a}^2}{R^2}\right)\end{aligned}\tag{80}$$

which together with (60) gives the effective action of the interacting vortex system.

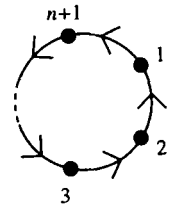

Fig. 5. Class of diagrams represented in Eq. (79).

We finally note that of course all loop diagrams in Figs. 4 and 5 can be calculated numerically to an arbitrary precision, but in view of the many approximations and qualitative arguments involved in our derivation of $\tilde{S}$ we considered the above rough estimation to be more adequate.

4.4. Vortex Phase Space Division and Effective Coulomb Gas Parameters

The result (80) of the last subsection already correctly defines the partition sum (15) of the vortex system. However, the unit of length in (15) is $\tilde{a}$ [which corresponds to R_c in Eq. (17)], so that in order to make the link to treatments of the neutral Coulomb gas in the literature we have to write the effective action in the form

$$\tilde{S}[\psi_0] = \frac{1}{T^{CG}} \sum_{i<j} m_i m_j \ln \frac{|\mathbf{R}_i - \mathbf{R}_j|}{\tilde{a}} + N \ln z^{CG} \tag{81}$$

whereas in (60) the original lattice spacing a appears in the logarithm. Then (81) defines the effective dimensionless Coulomb gas temperature T^{CG} and fugacity z^{CG}. Using the neutrality condition $\sum_i m_i = 0$ and the fact that $m_i = \pm 1$, we can rewrite the sum in (60) as

$$\sum_{i<j} m_i m_j \ln \frac{|\mathbf{R}_i - \mathbf{R}_j|}{a} = \sum_{i<j} m_i m_j \ln \frac{|\mathbf{R}_i - \mathbf{R}_j|}{\tilde{a}} - \frac{N}{2} \ln \frac{\tilde{a}}{a} \tag{82}$$

The second term will contribute to the fugacity z^{CG}, so we have to express $\tilde{a}$ as a function of the model parameters a, ξ. Recall that $\tilde{a}$ was an infrared cutoff on phase fluctuations defined so as to have the same effect as a mass $2/\xi^2$. To determine $\tilde{a}$ from this condition, note that the most important term in the perturbation series is (f) in Fig. 4 [and Eq. (74)] since it is the only one which contributes to the logarithmic vortex potential. Its size is mainly determined by the factor

$$\frac{K}{2} \langle |\psi_1|^2 \rangle = \frac{1}{4\pi} \ln \left(1 + 2\pi \frac{\xi^2}{a^2} \right) \tag{83}$$

calculated in (69). Now if one had chosen the "hard" momentum cutoff $\pi/\tilde{a}$ instead of the mass, the local fluctuations would have been given by

$$\frac{K}{2} \langle |\psi_1|^2 \rangle = \int_{\pi/\tilde{a} < k_{x,y} < \pi/a} \frac{d^2\mathbf{k}}{(2\pi)^2} \frac{1}{\mathbf{k}^2} \approx \frac{1}{4\pi} \int_{4\pi/\tilde{a}^2}^{4\pi/a^2} \frac{d(k^2)}{k^2} = \frac{1}{4\pi} \ln \frac{\tilde{a}^2}{a^2} \tag{84}$$

Identifying this expression with (83) leads to

$$\ln \frac{\tilde{a}}{a} = \frac{1}{2} \ln \left(1 + 2\pi \frac{\xi^2}{a^2} \right) \tag{85}$$

or, equivalently,

$$\tilde{a}^2 = a^2 + 2\pi\xi^2 \tag{86}$$

We insert (85) successively in (82), (60), (80) and obtain the required form (81) of the effective action, the Coulomb gas parameters now being given by the following expressions:

$$\frac{1}{T^{CG}} = 2\pi K - 2 \ln(1 + 2\pi X) \tag{87}$$

$$\ln z^{CG} = \frac{1}{2T^{CG}} \left\{ 2\mu_{XY} + F(X) - \frac{1}{2} \ln(1 + 2\pi X) \right\} + \frac{1}{2} \ln(1 + 2\pi X) + \frac{9\pi}{8} \frac{X}{1 + 2\pi X} \tag{88}$$

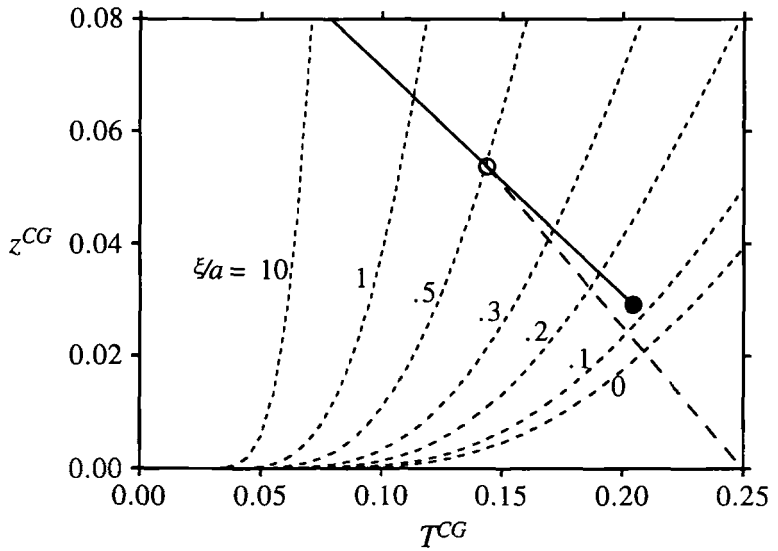

Fig. 6. Minnhagen's CG phase diagram as in Figs. 1 and 2, but now with our final $z^{CG}(T^{CG})$ relation for the GLCG [Eqs. (87), (88)], plotted for different values of ξ/a. The limit $\xi/a = 0$ corresponds to the XY model as shown in Fig. 1. With increasing ξ/a the $z^{CG}(T^{CG})$ line is shifted toward the upper part of the phase diagram, finally reaching the first-order part of the vortex unbinding transition.

where $2\mu_{XY} = -1.617$ [see Eq. (56)], $X = \xi^2/a^2$, and $F(X)$ is defined by Eq. (59).

Equations (87), (88) are the final results of this paper. The expression in curly brackets may be interpreted as a renormalized vortex chemical potential, whereas the second line of (88) contributes to the renormalized phase space division.

In Fig. 6 the z^{CG} vs. T^{CG} curves are drawn in Minnhagen's Coulomb gas phase diagram for different values of the GL correlation length ξ. With increasing ξ/a the curves cross the phase boundary at increasingly higher values of z^{CG}, finally reaching the first-order regime for values of $\xi \gtrsim a$. Since we argued in Section 2.1 that in superconducting films *always* $\xi \gtrsim a$, we conclude that the latter are good candidates for a first-order vortex unbinding transition. Because of the approximations and relatively rough estimations involved in our calculations we do not insist on the *quantitative* information conveyed by Fig. 6. However, we believe that the *trend* is clear enough to be reliable.

Another interesting (although not unexpected) result might be that for increasing ξ/a the transition occurs at increasingly higher values of K [which according to (3) corresponds to smaller values of the "physical" temperature]. In other words, the distance between T_v and T_{c0} increases with increasing ξ/a.

5. SUMMARY AND CONCLUSIONS

In this paper, we investigated the nature of the transition in the two-dimensional Ginzburg–Landau model of a neutral superfluid. In doing this, we assumed, as is usually done, that the transition is caused by the collective unbinding of vortex pairs. However, we paid particular attention to short-wavelength amplitude and phase fluctuations of the order parameter on length scales $\lesssim \xi$ (the Ginzburg–Landau correlation length), which we showed to be strongly coupled to the vortices. This is in contrast with previous work in the literature, where amplitude fluctuations usually are neglected altogether and phase fluctuations are assumed to be only weakly coupled to the vortices.

Eliminating perturbatively these short-wavelength fluctuations, we derived an effective free energy for the vortex degrees of freedom. We argued that this effective vortex gas still is a 2D Coulomb gas (i.e., the vortex–vortex interaction varies logarithmically at large distances); however, both the effective temperature and the fugacity of the Coulomb gas are strongly renormalized if ξ is larger than a microscopic cutoff length a for fluctuations. We argued that these considerations should be relevant for those

superconducting films for which a BCS description is qualitatively correct, since BCS theory predicts that *always* $\xi \gtrsim a$.

By this elimination process of small-scale fluctuations we furthermore obtained a microscopic interpretation of the effective vortex phase space division Δ as an interesting secondary result. In particular, we could clarify the relation between Δ and the Ginzburg–Landau correlation length ξ.

Our subsequent conclusions concerning a possible first-order transition then relied completely on the correctness of Minnhagen's self-consistent theory of a dense 2D Coulomb gas, which predicts a first-order vortex unbinding transition with nonuniversal (not KT-like) properties for sufficiently large values of the vortex fugacity ($z^{CG} \gtrsim 0.05$). Unfortunately, the rather subtle differences between a KT-like and a first-order vortex unbinding transition seem to be outside the scope of present experimental investigations of real superconducting films. However, we think that an interestingly and probably feasible (though likewise very hard) problem would be to investigate numerically the critical properties of a lattice Ginzburg–Landau model including fluctuating order parameter amplitudes.

ACKNOWLEDGMENTS

We thank D. Ariosa, D. Baeriswil, U. Eckern, F. Mila, and P. Minnhagen for clarifying discussions. One of us (D.B.) gratefully acknowledges financial support by the Swiss National Science Foundation.

REFERENCES

1. O. Penrose and L. Onsager, *Phys. Rev.* **104**:576 (1956); C. N. Yang, *Rev. Mod. Phys.* **34**:694 (1962).
2. N. D. Mermin and H. Wagner, *Phys. Rev. Lett.* **17**:1133 (1966); P. C. Hohenberg, *Phys. Rev.* **158**:383 (1967).
3. G. Lasher, *Phys. Rev.* **172**:224 (1968).
4. M. E. Fisher, M. N. Barber, and D. Jasnow, *Phys. Rev. A* **8**:1111 (1973).
5. D. J. Bishop and J. D. Reppy, *Phys. Rev. B* **22**:5171 (1980).
6. M. R. Beasley, J. E. Mooij, and T. P. Orlando, *Phys. Rev. Lett.* **42**:1165 (1979).
7. B. I. Halperin and D. R. Nelson, *J. Low Temp. Phys.* **36**:599 (1979).
8. A. F. Hebard and A. T. Fiory, *Phys. Rev. Lett.* **44**:291 (1980).
9. A. F. Hebard and A. T. Fiory, *Phys. Rev. Lett.* **50**:1603 (1983); A. T. Fiory, A. F. Hebard, and W. I. Glaberson, *Phys. Rev. B* **28**:5075 (1983).
10. C. Leemann, P. Flückiger, V. Marsico, J. L. Gavilano, P. K. Srivastava, P. Lerch, and P. Martinoli, *Phys. Rev. Lett.* **64**:3082 (1990).
11. S. Vadlamannatti, Q. Li, T. Venkatesan, W. L. McLean, and P. Lindenfeld, *Phys. Rev. B* **44**:7094 (1991).
12. V. L. Berezinskiĭ, *Zh. Eksp. Teor. Fiz.* **61**:1144 (1971) [*Sov. Phys. JETP* **34**:610 (1972)].
13. J. M. Kosterlitz and D. J. Thouless, *J. Phys. C* **5**:L124 (1972).
14. J. M. Kosterlitz and D. J. Thouless, *J. Phys. C* **6**:1181 (1973).

15. D. R. Nelson, in *Phase Transitions and Critical Phenomena*, Vol. 7, C. Domb and J. L. Lebowitz, eds. (Academic Press, London, 1983), p. 1.
16. N. R. Werthamer, in *Superconductivity*, R. D. Parks, ed. (Marcel Dekker, New York, 1969), p. 321; M. Cyrot, *Rep. Prog. Phys.* **36**:103 (1973).
17. B. I. Halperin, in *Physics of Low-Dimensional Systems*, Y. Nagaoka and S. Hikami, eds. (Progress of Theoretical Physics, Kyoto, 1979), p. 53.
18. R. P. Feynman, *Prog. Low Temp. Phys.* **1**:52 (1955); G. A. Williams, *Phys. Rev. Lett.* **59**:1926 (1987); **68**:2054 (1992); S. R. Shenov, *Phys. Rev. B* **40**:5056 (1989).
19. P. Minnhagen, *Rev. Mod. Phys.* **59**:1001 (1987).
20. J. M. Kosterlitz, *J. Phys. C* **7**:1046 (1974); P. B. Wiegmann, *J. Phys. C* **11**:1583 (1978); D. J. Amit, Y. Y. Goldstein, and G. Grinstein, *J. Phys. A* **13**:585 (1980).
21. J. V. José, L. P. Kadanoff, S. Kirkpatrick, and D. R. Nelson, *Phys. Rev. B* **16**:1217 (1977).
22. D. R. Nelson and J. M. Kosterlitz, *Phys. Rev. Lett.* **39**:1201 (1977).
23. P. Minnhagen and G. G. Warren, *Phys. Rev. B* **24**:2526 (1981).
24. W. Janke and K. Nather, *Phys. Lett. A* **157**:11 (1991).
25. A. Jonsson, P. Minnhagen, and M. Nylén, *Phys. Rev. Lett.* **70**:1327 (1993).
26. J. M. Caillol and D. Levesque, *Phys. Rev. B* **33**:499 (1986); J.-R. Lee and S. Teitel, *Phys. Rev. Lett.* **64**:1483 (1990); **66**:2100 (1991).
27. C. Leemann, P. Lerch, G. A. Racine, and P. Martinoli, *Phys. Rev. Lett.* **56**:1291 (1986); P. Martinoli, P. Lerch, C. Leemann, and H. Beck, In Proceedings of the 18th Conference on Low Temperature Physics, Kyoto 1987, *Jpn. J. Appl. Phys.* **26**:1999 (1987).
28. B. Jeanneret, P. Flückiger, J. L. Gavilano, C. Leemann, and P. Martinoli, *Phys. Rev. B* **40**:11374 (1989).
29. R. Pelcovits, Ph.D. Thesis, Harvard University (1978).
30. P. Minnhagen and M. Nylén, *Phys. Rev. B* **31**:5768 (1985).
31. P. Minnhagen, *Phys. Rev. B* **32**:3088 (1985).
32. J. M. Thyssen and H. J. F. Knops, *Phys. Rev. B* **38**:9080 (1988).
33. P. Minnhagen and M. Wallin, *Phys. Rev. B* **40**:5109 (1989).
34. A. P. Young, *J. Phys. C* **11**:L453 (1978).
35. H. Weber and P. Minnhagen, *Phys. Rev. B* **38**:8730 (1988).
36. F. Mila, *Phys. Rev. B* **47**:442 (1993).
37. L. P. Gor'kov, *Zh. Eksp. Teor. Fiz.* **36**:1918 (1959) [*Sov. Phys. JETP* **9**:1364 (1959)].
38. J. Pearl, *Appl. Phys. Lett.* **5**:65 (1964).
39. C. R. Hu, *Phys. Rev. B* **6**:1756 (1972).